The Company of
Biologists

RESEARCH ARTICLE

Hydrodynamic sensory threshold in harbour seals (*Phoca vitulina*) for artificial flatfish breathing currents

Benedikt Niesterok, Guido Dehnhardt and Wolf Hanke*

ABSTRACT

Harbour seals have the ability to detect benthic fish such as flatfish using the water currents these fish emit through their gills (breathing currents). We investigated the sensory threshold in harbour seals for this specific hydrodynamic stimulus under conditions which are realistic for seals hunting in the wild. We used an experimental platform where an artificial breathing current was emitted through one of eight different nozzles. Two seals were trained to search for the active nozzle. Each experimental session consisted of eight test trials of a particular stimulus intensity and 16 supra-threshold trials of high stimulus intensity. Test trials were conducted with the animals blindfolded. To determine the threshold, a series of breathing currents differing in intensity was used. For each intensity, three sessions were run. The threshold in terms of maximum water velocity within the breathing current was 4.2 cm s^{-1} for one seal and 3.7 cm s^{-1} for the other. We measured background flow velocities from 1.8 to 3.4 cm s^{-1}. Typical swimming speeds for both animals were around 0.5 m s^{-1}. Swimming speed differed between successful and unsuccessful trials. It appears that swimming speed is restricted for the successful detection of a breathing current close to the threshold. Our study is the first to assess a sensory threshold of the vibrissal system for a moving harbour seal under near-natural conditions. Furthermore, this threshold was defined for a natural type of stimulus differing from classical dipole stimuli which have been widely used in threshold determination so far.

KEY WORDS: Vibrissae, Sensory system, Benthic fish, Hydrodynamic stimulus, Pinniped, Signal-to-noise ratio

INTRODUCTION

Harbour seals possess prominent vibrissae which function as a hydrodynamic sensory system. To assess the sensitivity of this system, absolute thresholds have been determined experimentally using hydrodynamic dipole stimuli generated with spheres that oscillate sinusoidally in the water. In the dipole flow field generated by a sinusoidally oscillating sphere of 10 cm diameter, harbour seals detect flow velocities as low as 245 μm s^{-1} at 50 Hz, the oscillation frequency of best sensitivity (Dehnhardt et al., 1998). The absolute sensitivity of the vibrissal system is therefore comparable to the sensitivity found for the hydrodynamic sensory systems in teleost fish (Bleckmann and Münz, 1990; Bleckmann et al., 1981), crustaceans (Tautz and Sandemann, 1980) or cephalopods (Budelmann and Bleckmann, 1988). However, the hydrodynamic sensory system

(lateral line system) of some fish is 10–100 times more sensitive to hydrodynamic dipole stimuli (Bleckmann et al., 1989; Coombs and Janssen, 1990) compared with the vibrissal system of harbour seals.

All these studies deal with absolute sensitivities lacking the influence of hydrodynamic noise, such as that produced by flow over the animal as it swims and background flow from external sources. However, the capability of a sensory system in nature must be studied under the influence of background noise. So far, this has been done in fish to some extent. Engelmann et al. (2002) recorded the responses of primary lateral line afferent fibres to a stationary vibrating sphere in running water. They showed that the electrophysiological response pattern of the superficial neuromasts in goldfish is masked in running water in comparison to the same stimulus in still water. The response pattern of canal neuromasts is barely affected by running water for this stimulus type. The lateral line canal therefore acts as a high-pass filter, filtering out the background noise that running water constitutes. This filter function is also maintained on a higher neuronal hierarchy level in the medial octavolateral nucleus (Kröther et al., 2002), which is a primary site for hydrodynamic information processing in the brainstem of fish. These two studies used electrophysiological methods. Only one behavioural study on the capability of the lateral line system in fish under the influence of background noise has so far been conducted (Bassett et al., 2006). It confirmed that the orientation towards a dipole stimulus in a fish with an extensive array of superficial neuromasts was severely impaired in background flow. However, the sensory threshold of hydrodynamic sensory systems to more natural stimuli under the influence of natural hydrodynamic background noise and self-motion has not yet been studied.

In our previous study (Niesterok et al., 2017), we demonstrated a harbour seal's ability to detect artificial breathing currents using its vibrissae under the influence of hydrodynamic background noise and self-motion. Here, we used artificial flatfish breathing currents to investigate the efficiency of the vibrissal system in terms of a threshold for this specific hydrodynamic stimulus under the influence of self-motion and background noise.

MATERIALS AND METHODS
Experimental animals
This study was conducted with two male harbour seals (*Phoca vitulina* Linnaeus 1758), Henry and Luca, which had also participated in our former experiment on the detection of artificial flatfish breathing currents (Niesterok et al., 2017). They were 19 years (Henry) and 13 years (Luca) old. Both seals received more than 90% of their daily ration of food (herring and sprats) during the experiments. The experiments were carried out in accordance with the European Communities Council Directive of 24 November 1986 (86/609/EEC).

Experimental setup
The experimental setup used for this study was similar to that in our previous study (Niesterok et al., 2017), with some modifications

University of Rostock, Institute for Biosciences, Department of Sensory and Cognitive Ecology, Albert-Einstein-Straße 3, 18059 Rostock, Germany.

*Author for correspondence (wolf.hanke@uni-rostock.de)

W.H., 0000-0003-1682-4525

Journal of Experimental Biology

(Fig. 1). In brief, a platform was suspended 1 m below the water surface. Eight nozzles to produce the artificial breathing currents were mounted at eight different positions, spaced 110 cm lengthwise and 135 cm crosswise apart. Each nozzle was connected to a tube below the platform. Water flow through the tubes and the nozzles was produced by a gear pump operated at predefined rotational speeds. One nozzle at a time was active; the active nozzle was selected by manually operating eight ball valves between the gear pump and the eight tubes. Nozzles emitted water currents at an angle of 45 deg to the platform, approximating the angle at which a flatfish's breathing current emerges from the substrate. A horizontal mesh wire grid prevented the animals from approaching the nozzle closer than 23 cm. A top camera and one underwater lateral camera per nozzle filmed the animals.

In the present study, the orientations of nozzles 4 and 5 were changed by 90 deg so that breathing currents were directed along the short side of the platform (Fig. 1A). The sites where breathing currents crossed the mesh wire grid and therefore were potentially detectable by the experimental animals were marked using blue PVC rings (outer diameter 30 cm) that were visible in the top camera view. These markings served to assist in deciding whether the seal had crossed the site of the hydrodynamic stimulus (seal snout crossed the blue ring or was even in its centre) and whether it stationed correctly in the case of a positive response. The side view cameras and the top view camera were used to decide whether the

animal crossed the site of the breathing current and whether the animal gave a clear behavioural response (see 'Experimental procedure', below).

While the opening of the nozzles was just below the mesh wire grid in our previous study (Niesterok et al., 2017), for this experiment the openings of the nozzles were lowered (Fig. 1B) by 23 cm vertically, to imitate another potential situation in the wild: a seal swimming over the ground at some distance. This way, it was also ensured that stimuli in the range around the threshold were reproducible, as extremely low rotational speeds of the pump, which tended to affect reproducibility, were avoided. The distance from the opening of the nozzles to the site where the artificial breathing current crossed the mesh wire grid was 36 cm (Fig. 1B).

Hydrodynamic stimuli

Different rotational speeds (measured in revolutions per minute, rpm) of the motor were applied to generate different stimulus intensities in order to approach the sensory thresholds of the harbour seals. Rotational speeds of 200, 100, 80, 70 and 60 rpm were used, and their flow fields were quantified using particle image velocimetry (PIV) (Westerweel, 1997). The flow field measurements were conducted in the netted enclosure (an enclosure separated from the marine environment only by a net) where the experimental setup was installed. The same measurement device was used as in the background flow measurements in our previous
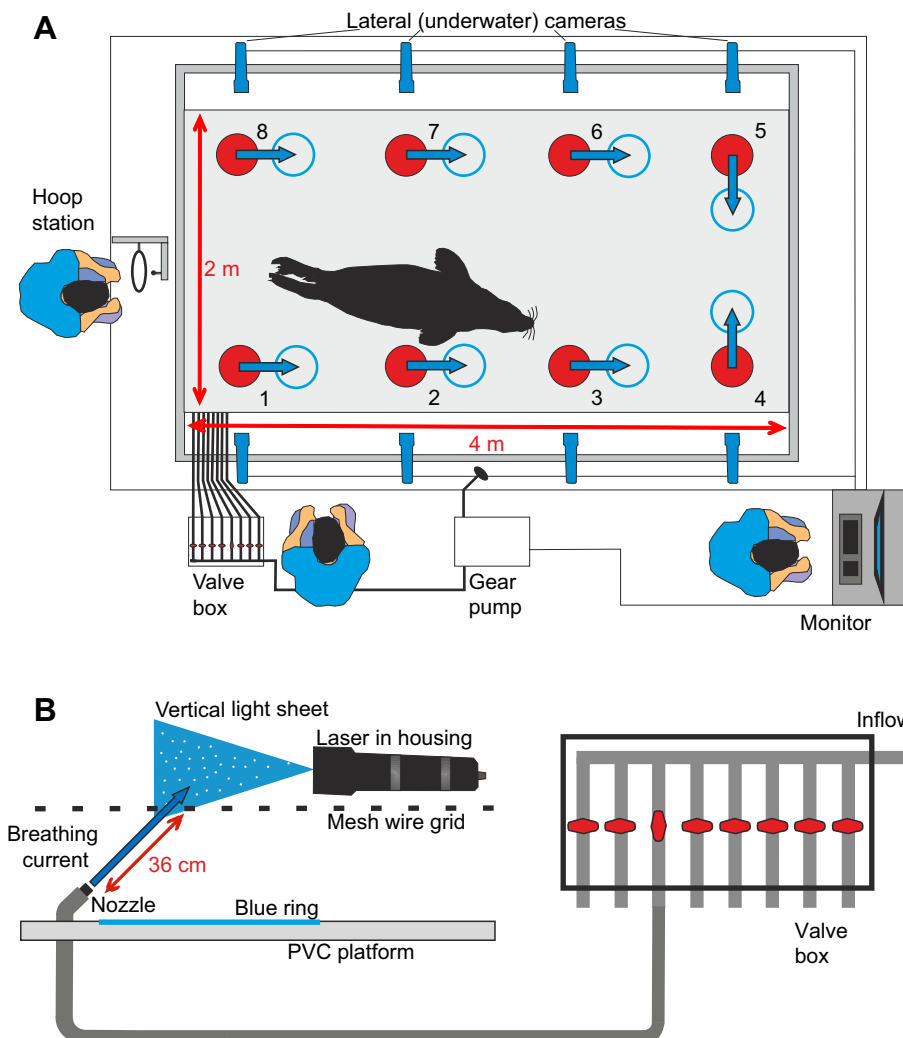

Fig. 1. Experimental setup. (A) Top view. The positions of the nozzles are marked with red circles. The points where the breathing currents crossed the grid are marked with blue rings; the flow direction of the emitted breathing current is indicated by a blue arrow for each nozzle. (B) Overview of the experimental setup from the valve box to the emitted breathing current; the opening of the nozzle is located 25 cm below the mesh wire grid; the breathing current extends over a distance of 36 cm before crossing the grid, marked with a blue ring attached to the platform below. The laser sheet and laser housing of the particle image velocimetry (PIV) device are also shown. The laser sheet is oriented vertically.

study (Niesterok et al., 2017) with one modification: the measurement plane defined by the laser light sheet was vertical, intersecting with the opening of the nozzle (Fig. 1B). The camera field of view recorded particle movements above the mesh wire grid as this was the area where the seal was allowed to swim. Artificial seeding particles were added to the water in front of the intake socket of the gear pump. This way, particles were transported through the hose system and emitted from the nozzles. A sequence of 100 frames (2 s) for each stimulus intensity was used for water velocity calculation. We considered each sequence representative as we conducted flow measurements on a day that did not differ from the other experimental days in terms of weather conditions. For each frame, the mean flow velocity of the 10 strongest vectors was calculated. From these, the temporal mean over all frames was calculated. The resulting flow velocities for each rotational speed (200, 150, 100, 80, 70 and 60 rpm) of the motor were finally fitted with a quadratic function to relate rotational speed to flow velocity.

Experimental procedure

The basic procedure of a trial was the same as in our previous study (Niesterok et al., 2017). Each session consisted of 24 trials. These 24 trials were composed of supra-threshold trials with a stimulus intensity of 7.4 cm s^{-1} (200 rpm) and test trials of a particular stimulus intensity [7.4 cm s^{-1} (200 rpm), 4.9 cm s^{-1} (100 rpm), 3.8 cm s^{-1} (80 rpm), 3.2 cm s^{-1} (70 rpm), 2.6 cm s^{-1} (60 rpm)]. Only one stimulus intensity was presented as a test trial in a session. For stimulus intensities of 7.4 and 4.9 cm s^{-1}, 12 test trials were conducted within a session. Two sessions were conducted for each of these two stimulus intensities. For stimulus intensities of 3.8, 3.2 and 2.6 cm s^{-1}, three sessions were run for each intensity, with eight test trials per session. This resulted in a total of 24 trials for each stimulus intensity. The animal was blindfolded for all test trials to exclude visual cues. The remaining trials (supra-threshold trials with an intensity of 7.4 cm s^{-1}) within a session were a mixture of blindfolded and non-blindfolded trials. The supra-threshold trials served to provide a high success rate for the animal in order to maintain its motivation. The experimental animals had to fulfil a minimum performance of 75% correct detections (baseline) for these supra-threshold trials for the session to be included in the analysis.

In the first sessions, we conducted training trials with stimulus intensities even higher than the highest intensity for the test trials. In these training sessions, the seals detected more than 75% of the breathing currents. This step was introduced to guarantee that the animals were well trained for this task. We then continued with two sessions using test stimuli of 7.4 cm s^{-1} only, and as these were detected reliably, we introduced test stimuli of 4.9 cm s^{-1} in the following session, using 7.4 cm s^{-1} for supra-threshold trials. The other stimulus intensities were presented in the subsequent sessions in a randomized order, with one stimulus intensity tested per session, combined with 7.4 cm s^{-1} supra-threshold trials. This was to prevent the animal from learning that stimulus intensity decreases with increasing number of sessions and changing its behaviour based on that cue. The procedure used here can be considered a modified method of constant stimuli, as different stimulus intensities were presented randomly not within a session but session-wise.

The top view camera from the previous study (Niesterok et al., 2017) was again used to reliably judge whether the animal crossed the site of the hydrodynamic stimulus or not. The muzzle of the animal had to intersect the blue ring on the experimental platform.

The blue rings marked the sites where the breathing currents crossed the mesh wire grid. If the experimental animal did not cross the breathing current, the trial was repeated until the animal crossed the site and therefore had the chance to sense the stimulus.

Performance and threshold

The performance of each animal for each stimulus intensity was calculated as the overall proportion of successful trials with respect to all trials of a particular intensity (24 trials, performed in 2–3 sessions). Measured flow velocities were plotted over rotational speeds of the pump and fitted with a quadratic function to link each rotational speed to a flow velocity. Flow velocities derived from the quadratic function were correlated to the performance of each animal.

The performances of both seals were plotted over flow velocities and fitted with quadratic functions. As there were eight different sites at which the animals could respond correctly, but the animal was not limited to responding at these sites, the probability of finding the correct nozzle by mere chance was below 0.125. This results in 7 successful trials out of 24 trials (29%) to be significant at a level of 5%. Using the quadratic model between flow velocity and animal performance, the corresponding flow velocity for a performance of 29% was calculated as the threshold.

The performance for nozzles 1–4 (seals swimming along with the emitted breathing current) was compared with the performance at nozzles 5–8 (seals swimming against the emitted breathing current) using an exact Fisher test. The performance at the following stimulus intensities was considered for statistics: 70, 80, 100 and 200 rpm.

Measurement of background flow velocity and calculation of signal-to-noise ratio

Background velocities were measured using the PIV device described in Niesterok et al. (2017). The movement of naturally occurring particles in a laser light sheet was recorded in a representative location next to the frame of the setup. The laser light sheet was at the same level as the mesh wire grid, which is the level where the animals were allowed to search for the breathing current. For each experimental day, three sequences were chosen for evaluation from these recordings based on particle density. Only recordings from sessions with stimulus intensities of 3.2, 3.8 and 4.9 cm s^{-1} were used, as those were the sessions close to the detection threshold. Altogether, background flow velocities from seven sessions could be evaluated for each animal.

Stimulus intensities at threshold were calculated from the quadratic function between rotational motor speed and flow velocity. Hydrodynamic background flow was averaged across sessions for each animal. Signal-to-noise ratio was calculated as the ratio of these two values for each animal.

Swimming speed

Swimming speed was evaluated similar to our previous study (Niesterok et al., 2017). The same camera and tracking software were used. However, in the present study only test trials (trials where the test stimulus was presented) were evaluated. All test trials were blindfolded trials, in which the animal either succeeded in sensing the stimulus or not. Some test trials could not be evaluated for technical reasons (e.g. light reflections in the corner positions). Swimming speeds in test trials with stimulus intensities near the threshold (3.8 and 4.9 cm s^{-1}) and far above the threshold (7.4 cm s^{-1}) were measured.

Statistics

Statistics were run in R (R Development Core Team 2008) and Matlab (MATLAB and Statistics Toolbox Release 2012b, The MathWorks, Inc., Natick, MA, USA).

RESULTS

Detection rate of hydrodynamic stimulus and threshold

The correlation between the rotational speed of the motor and the corresponding mean flow velocity is shown in Fig. 2.

The performance at each stimulus intensity tested for each animal is presented in Fig. 3, along with the quadratic fitting function. The course of the graphs is similar for the two seals. They show similar performance for flow velocities of 2.6, 3.2 and 4.9 cm s^{-1} but differ in their performance at flow velocities of 3.8 and 7.4 cm s^{-1}.

The hydrodynamic sensory threshold for this type of stimulus for Henry was 4.2 cm s^{-1} (red line in Fig. 3A); for Luca, the threshold was 3.7 cm s^{-1} (red line in Fig. 3B).

Statistical analysis (exact Fisher test) did not reveal any differences in the performance of the two animals when swimming with (nozzles 1–4) or against (nozzles 5–8) the breathing current. This result proved to be true for the stimulus intensities above the threshold (4.9 and 7.4 cm s^{-1}) as well as for the stimulus intensities below the threshold (3.2 and 3.8 cm s^{-1}; Table 1); at 2.6 cm s^{-1}, the seals never detected the stimulus.

Hydrodynamic background noise

Hydrodynamic background noise ranged from 2.4 to 3.4 cm s^{-1} in the sessions with Henry and from 1.8 to 3.4 cm s^{-1} in the sessions with Luca. Therefore, hydrodynamic background flow was comparatively stable across sessions. There were no sessions with remarkably high wind speeds. The average background noise across sessions was 2.9 cm s^{-1} for Henry and 2.5 cm s^{-1} for Luca. The calculated signal-to-noise ratios at the respective thresholds were 1.4 for Henry and 1.5 for Luca. Therefore, as a rule of thumb, both seals detected the breathing currents successfully at a stimulus 1.5 times higher than the background noise in terms of flow velocity. The best signal-to-noise ratio was found for Luca on a day with a background noise of 3.4 cm s^{-1} and a stimulus strength of 3.8 cm s^{-1}.

Swimming speed

The two harbour seals differed in their swimming speed. Henry swam at speeds ranging from 19 to 62 cm s^{-1} with a mean of 40 cm s^{-1}. Luca swam at speeds ranging from 33 to 95 cm s^{-1} with a mean of 69 cm s^{-1}. There was no significant difference between the swimming speeds in test trials at stimulus intensities of 3.8 and

Table 1. Results of exact Fisher test

Stimulus intensity (cm s^{-1})	P-value	
	Luca	Henry
3.2	1	1
3.8	0.68	0.32
4.9	1	0.21
7.4	1	0.77

P-values are above the significance level of $\alpha=0.05$ and indicate no difference between the animals' performances in finding the breathing current when swimming with or against it. All values above significance level indicate no difference between the animal's performance in finding the breathing current when swimming with or against it.

4.9 cm s^{-1} for the two seals (t-test; P=0.4089 for Luca; P=0.2159 for Henry; Fig. 4A,C).

However, comparing swimming speeds of successful trials with those of unsuccessful trials at stimulus intensities of 3.8 and 4.9 cm s^{-1}, i.e. at the stimulus intensities around threshold, significant differences of the means of swimming speeds were found for both animals (t-test; P=0.0131 for Luca; P=0.0003 for Henry; Fig. 4B,D). Descriptive statistics on swimming speeds for all four cases (3.8 and 4.9 cm s^{-1}, successful trials and unsuccessful trials) are shown in Table 2 for seals Henry and Luca. Another comparison between swimming speeds at stimulus intensities of 3.8 and 4.9 cm s^{-1} (around threshold) and swimming speeds at the stimulus intensity of 7.4 cm s^{-1} (far above threshold) did not reveal any significant differences (t-test; P=0.205 for Henry; P=0.02534 for Luca). At the higher stimulus intensity of 7.4 cm s^{-1}, Luca's swimming speeds ranged from 33 to 78 cm s^{-1}, and Henry's swimming speeds ranged from 22 to 60 cm s^{-1} (also included in Table 2). Significant differences
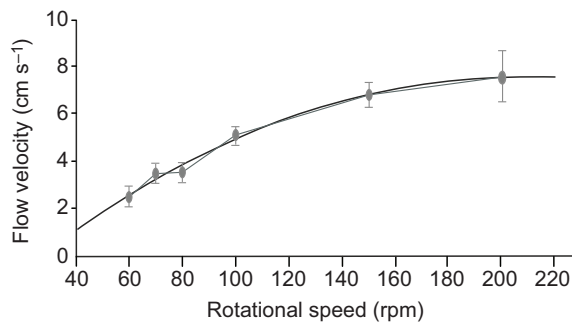
Fig. 2. Correlation between the rotational speed of the pump and the corresponding mean flow velocity. Flow velocity was measured at the level of the grid in the setup. The grey line connects the mean data points (±s.d.); the black line represents the quadratic fit.
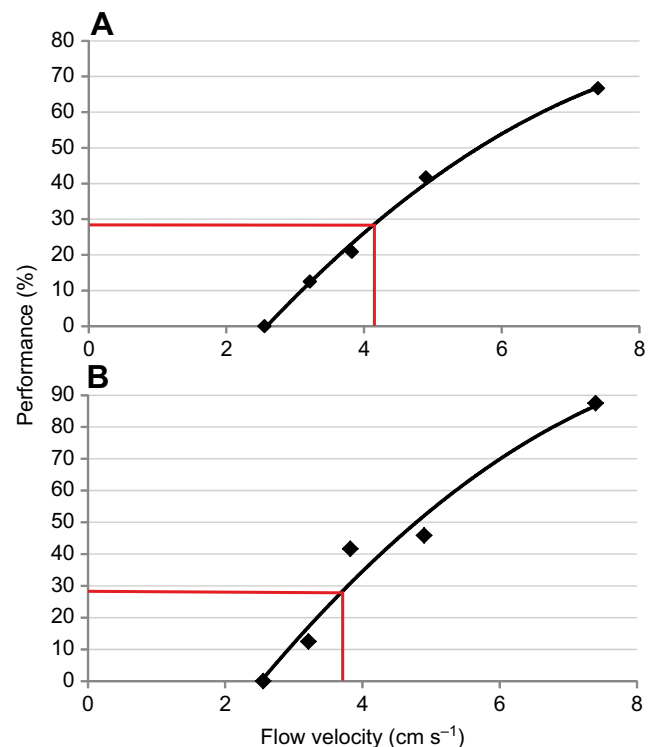
Fig. 3. Correlation between performance and stimulus intensity. Stimulus intensity is given as mean flow velocity at different rotational speeds of the pump. Black lines represent the fitted functions; red lines mark the corresponding thresholds at the significant performance of 29%. (A) Data for seal Henry; (B) data for seal Luca.

Table 2. Overview of descriptive statistics on the swimming speed of seals Luca and Henry

	Luca					Henry				
	3.8 cm s⁻¹	4.9 cm s⁻¹	7.4 cm s⁻¹	Successful	Unsuccessful	3.8 cm s⁻¹	4.9 cm s⁻¹	7.4 cm s⁻¹	Successful	Unsuccessful
Swim speed (cm s⁻¹)										
Minimum	33	53	33	33	56	22	19	22	19	32
Mean	70	67	61	63	73	43	37	36	31	46
Maximum	95	94	78	77	95	62	62	60	51	62
s.d.	13	12	11	11	12	12	12	11	10	10

Swimming speeds are displayed separately for different stimulus intensities (=flow speeds: 3.8, 4.9 and 7.4 cm s⁻¹) and for successful (at flow speeds of 3.8 and 4.9 cm s⁻¹) and unsuccessful (at flow speeds of 3.8 and 4.9 cm s⁻¹) trials. The statistical parameters of the distributions under each condition are minimum swimming speed, maximum swimming speed, mean and standard deviation of the respective distribution of swimming speeds.

between swimming speeds in successful and unsuccessful trials at a stimulus intensity of 7.4 cm s⁻¹ were not found.

DISCUSSION
Detection rates and threshold
The thresholds were similar in the two seals (3.7 and 4.2 cm s⁻¹), which underscores the validity of the thresholds. The thresholds determined in this experiment differ greatly from other thresholds (see Introduction) for the detection of hydrodynamic events. Compared with the absolute threshold of 245 µm s⁻¹ (at 50 Hz) in the study of Dehnhardt et al. (1998) for the vibrissal system of a harbour seal, the thresholds in this study are 150 times and 170 times higher. However, the flow field of the oscillating sphere

(hydrodynamic dipole) in the study of Dehnhardt et al. (1998) differs greatly from the flow field of a breathing current in its overall structure, and temporal and spatial extent. While the flow pattern around the sinusoidally oscillating sphere changes its direction sinusoidally with the same oscillation frequency, the breathing current flows in one primary direction. The duration of the stimulus was significantly shorter in the present experiment, as the swimming seal encountered the breathing current for less than 0.5 s, while the dipole stimulus in the study of Dehnhardt et al. (1998) lasted 3 s. The breathing current in the present study stimulated only some of the vibrissae, whereas all of the vibrissae were stimulated by the dipole. The frequency of the hydrodynamic stimulus differs in the two studies: in the dipole experiment (Dehnhardt et al., 1998), pure
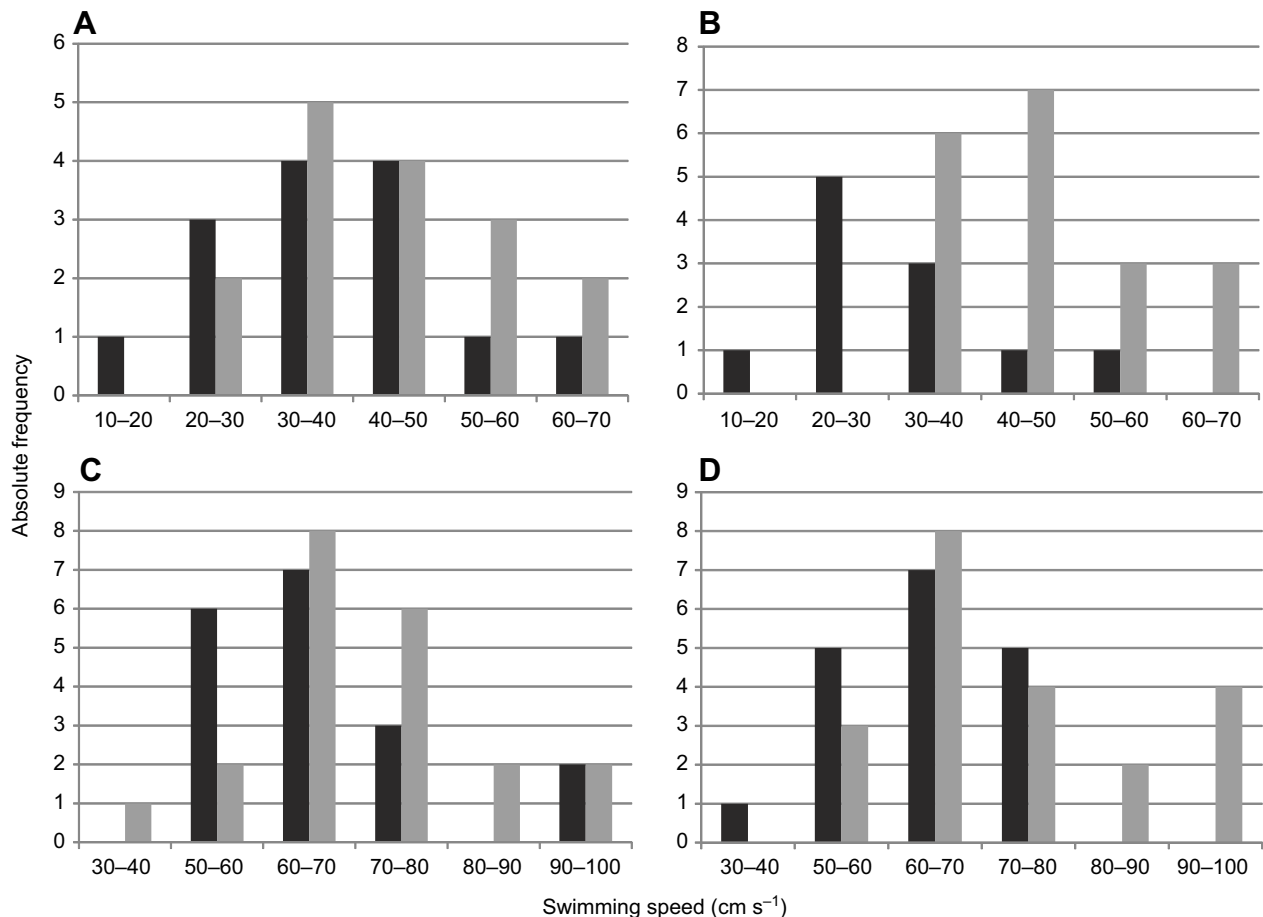

Fig. 4. Overview of frequency distribution of swimming speed. (A) Swimming speeds performed by seal Henry for all trials (successful and unsuccessful) with a stimulus intensity of 3.8 cm s⁻¹ (black bars) and 4.9 cm s⁻¹ (grey bars). (B) Swimming speeds performed by seal Henry for all trials with stimulus intensities of 3.8 and 4.9 cm s⁻¹ differentiated by successful trials (black bars) and unsuccessful trials (grey bars). (C,D) As for A and B, for seal Luca.

frequencies were used, and the lowest detection threshold was found at 50 Hz. The frequency content of the breathing current in the present study is a result of the interaction of the swimming movement and the predominantly unidirectional water current from below, and will contain a broader spectrum of frequencies, presumably mostly below 50 Hz.

In the dipole study by Dehnhardt et al. (1998), hydrodynamic background noise was not quantified, but was probably in the very low frequency range, while the stimuli ranged from 10 to 100 Hz. Masking of the hydrodynamic stimulus by background noise will probably be largely ineffective with such a difference in frequencies, as has been well studied in the acoustic system (reviewed in Erbe et al., 2016; Fletcher, 1940). In the present study, hydrodynamic background noise was present and was quantified in order to assess the seal's performance under natural conditions.

Hydrodynamic background noise

Background noise is a factor to be considered in the interpretation of experimental sensory thresholds. The present study provides the first sensory threshold for a vibrissal system under natural background noise conditions. Two distinctly different types of background noise were present: the natural water flow in the open air enclosure and the noise introduced by the animal's active swimming movements.

Natural water flow was measured with PIV in a horizontal layer in the experimental enclosure after the experimental sessions. The range of flow velocities was not unusual: they matched the flow velocities in our previous study (Niesterok et al., 2017) and the flow velocities we observed as background noise when measuring the artificial breathing currents in our setup.

The best approach to calculate the signal-to-noise ratio in this behavioural experiment would be background noise measurement at the position where and at the instant when the animal receives the stimulus, but for technical reasons this has not been implemented yet. Hydrodynamic background noise may have been higher than the background noise measured daily after the conclusion of the experiments, at least in part of the trials, as a seal swimming within the limited enclosure causes water movements that will last for a considerable time (Schulte-Pelkum et al., 2007). In addition, occasionally fishes entered the netted enclosure and could have added hydrodynamic background noise.

To characterize the efficiency of a hydrodynamic sensory system, the ratio between a hydrodynamic event (the signal) and the hydrodynamic background noise can be calculated. This signal-to-noise ratio has not yet been quantified for the mammalian vibrissal system; the present study provides a first approach.

The best signal-to-noise ratio of 1.1 was calculated from absolute values of 3.4 cm s^{-1} (noise) and 3.8 cm s^{-1} (signal or stimulus). If that flow velocity of the hydrodynamic background noise was really present at the moment of detection, this small difference of 0.4 cm s^{-1} would be sufficient for successful detection; however, background flow was measured only after the experimental session.

A factor that will facilitate the detection of the breathing current in the presence of background flow in the same order of magnitude is the directional information. While background noise mainly consisted of a lateral water movement in the horizontal plane, the breathing currents were directed upwards at an angle of 45 deg to the ground. Thus, there was a vertical component striking the animals' vibrissae while they were constantly exposed to predominantly horizontal background noise. The contribution of the vertical flow component to the sensation of a breathing current is probably significant. Harbour seal vibrissae are flattened in cross-section,

with the narrow side facing the oncoming flow during forward swimming and the broad side facing the sea bottom (B.N., G.D. and W.H., personal observation). It is known that flow from the broad side of the flattened vibrissa displaces a single vibrissa more than flow from the narrow side (Murphy et al., 2013). The vibrissae of a swimming harbour seal appear ideally suited to detect water flow in a vertical direction, as exemplified by the breathing currents studied here.

Background noise from vortex-induced vibrations generated by self-motion

A second type of background noise that affects detection thresholds in the actively swimming animal will be produced by the movement of the vibrissae through the flow. Behind a cylinder-like object such as a vibrissa in a flow with Reynolds numbers above approximately Re=50, vortices are shed that exert forces on the object. The vortices cause the cylinder to vibrate, an effect known as vortex-induced vibration. However, harbour seal vibrissae possess an undulated shape that reduces vortex-induced vibration by more than 90% (Hanke et al., 2010). This effect will be most pronounced when flow impinges from the narrow side of the flattened vibrissa, i.e. in the swimming direction of the animal, and appears to be designed to suppress vortex-induced vibrations caused by forward swimming.

In a biomimetic study, Miersch et al. (2011) investigated three vibrissae of a harbour seal (*Phoca vitulina*) and three vibrissae of a California sea lion (*Zalophus californianus*) for the ratio of the vortex-induced vibrations caused by flowing water and a hydrodynamic signal consisting of the wake of an object immersed in the water. Vibrissae of each species were immersed one at a time into the water of a rotating flow channel. The hair shaft was fixed in a piezoceramic cylinder above the water surface, which transformed the oscillating movement of the hair shaft to electrical voltage. Measurements were conducted with a cylinder in front of the hair inside the water (signal) and without a cylinder (noise). The resulting mean signal-to-noise ratios were 2.2 in harbour seal vibrissae and 0.36 in California sea lion vibrissae, underlining effective suppression of vortex-induced vibrations in harbour seal vibrissae in comparison to the less-specialized sea lion vibrissae.

We conclude that background noise due to vortex-induced vibrations is minimized by the design of harbour seal vibrissae in a setting such as the detection of breathing currents.

Swimming speed

The swimming speeds of the animals ranged from 19 to 95 cm s^{-1}. This range is comparable with the estimated swimming speeds found in studies on hydrodynamic trail following in harbour seals (Dehnhardt et al., 2001; Hanke et al., 2010; Wieskotten et al., 2010) and measured values from our previous study on benthic breathing current detection (Niesterok et al., 2017). As we did not find any differences in swimming speeds at the higher flow intensity in comparison to the stimulus intensities around threshold, we conclude that the animals did not know which intensity was tested in a session and therefore could not adjust their swimming speed.

At the high stimulus intensity (7.4 cm s^{-1}), no differences in swimming speeds between successful and unsuccessful trials were found. For this stimulus intensity, the swimming speeds of the seals did not affect their detection of the artificial breathing current.

Interestingly, when testing stimulus intensities around threshold, swimming speeds for successful trials differed significantly from swimming speeds of unsuccessful trials. Swimming speeds in successful trials ranged from 19 to 51 cm s^{-1} for Henry and from 33 to 77 cm s^{-1} for Luca and were significantly lower than swimming speeds in unsuccessful trials. We conclude that swimming speed is a

factor that has an influence on successful detection of a breathing current close to the threshold. Two conceivable explanations for this effect are a possible increase of vortex-induced vibrations with swimming speed, and the reduced duration of stimulus encounter when the seal swims through the breathing current more quickly.

Vortex-induced vibrations are largely reduced in harbour seal vibrissae (Hanke et al., 2010). Miersch et al. (2011) measured vortex-induced vibrations of single vibrissae mounted in a flow tank at flow velocities from 15 to 55 cm s^{-1} and found no indication of an increase of vibration amplitude (although there was an increase in vibration frequency). As this flow velocity range approximates the swim speeds of the seals in the present study, we consider it unlikely that vortex-induced vibrations caused the reduced success rate with increased swim speeds observed here.

Stimulus duration may affect the sensory threshold, at least within limits. For example, this effect is well known in the acoustic system, where an increase in stimulus duration up to a limit of several hundred milliseconds lowers the sensory threshold (Clack, 1966; Popov and Supin, 1990). In the present study, the seal's vibrissal array usually passed the area of the breathing current in less than 0.5 s. Lower swimming speeds, i.e. longer stimulus durations, may increase success rate via a similar effect.

In conclusion, it should be advantageous for a seal not to swim 'too fast' when trying to detect a hydrodynamic stimulus. We hypothesize that there is an upper limit of swimming speed for a harbour seal for the successful detection of a breathing current close to the threshold.

Ecological implications

In the present study, the distance of the seal from the nozzle that emitted the artificial breathing current was greater than in our previous study (Niesterok et al., 2017), as the seal had to stay above a mesh wire grid 25–26 cm (previously 2–3 cm) above the nozzle. Our previous study mimicked the breathing currents of flounders of 16 cm body length. These breathing currents would drop to 2–2.5 cm s^{-1} at the new, increased distance (extrapolated values). The seals' sensory thresholds found in the present study were 3.7 and 4.2 cm s^{-1}. Assuming that breathing currents of flatfish scale approximately linearly with size, it can be concluded that harbour seals hunting for flatfish in the wild at some distance over the sea bottom rely on breathing currents of larger flounders than the ones imitated in our previous study (Niesterok et al., 2017). Flatfish imitated in the present study would be approximately 1.5–2 times as long as in the previous study, i.e. 24–32 cm. The relationship between breathing current strength and size of a flatfish should be investigated. However, we observed that our artificial breathing currents (Niesterok et al., 2017) match the real breathing current of a real flounder (Niesterok et al., 2017) not only in terms of the flow velocities right at the nozzle opening/gill opening but also in the way the flow velocities decay from their corresponding origin (nozzle opening/gill opening). This is a good indication that the artificial breathing current with increased flow velocity matches the breathing current of a bigger flounder very well. A study by Hughes (1966) confirms an increase of water flow through the gills with increasing body size in fish (smallmouth bass, *Micropterus dolomieu*).

Two different directions of the breathing currents in relation to the seal's swimming direction were used: with or against the seal's swimming direction. As no significant differences were found for these two conditions, we conclude that harbour seals are able to detect flatfish of appropriate size approaching from different directions, even when they swim over the ground at some distance.

Comparison with hydrodynamic sensing in fishes

The lateral line system in fish can have lower thresholds for dipole stimuli than those of the harbour seal in the study by Dehnhardt et al. (1998) by a factor of 10 (Bleckmann et al., 1989) and 100 (Coombs and Janssen, 1990). These studies measured responses from stationary animals at defined frequencies. The experiments on fish were conducted in laboratory tanks and the study on harbour seals was conducted in a confined pool, where hydrodynamic background noise in the respective frequency range was reduced and probably negligible.

In a study by Schwalbe et al. (2016), trained cichlids (*Aulonocara stuartgranti*) responded to artificial benthic hydrodynamic stimuli at flow velocities down to 1 mm s^{-1}. This flow velocity is far below the threshold found for harbour seals in the present study. However, fish were not visually restricted and background flow was probably less than in our near-natural setup. The most accurate available sensory threshold for harbour seals in terms of flow velocity at low frequencies, although obtained with a different setup, is the threshold for dipole stimuli at an oscillation frequency of 10 Hz presented in Dehnhardt et al. (1998), which is 1.8 mm s^{-1}.

Conclusions and outlook

This study is the first to quantify the sensory threshold of hydrodynamic perception with the vibrissal system in a near-natural setting and in an ecologically relevant task that parallels natural feeding behaviour. To date, dipole stimuli have been used widely for defining hydrodynamic sensory thresholds. The present study provides a hydrodynamic sensory threshold based on a new stimulus: breathing currents. While thresholds based on dipole stimuli and stationary experimental animals provide a valuable baseline and the opportunity to investigate pure stimulus frequencies, breathing currents presented to naturally behaving animals are representative of stimuli in the natural habitat, and the performance of the sensory system under these conditions gives insight into the performance of the sensory system in the wild. To gain a comprehensive understanding of the capability of the vibrissal system, various ecologically relevant stimuli should be tested along with naturally occurring factors (hydrodynamic background noise, self-motion), which can influence prey detection. For this reason, more comparative studies in addition to experiments under controlled conditions should be carried out in the open sea.

References
Bassett, D. K., Carton, A. G. and Montgomery, J. C. (2006). Flowing water decreases hydrodynamic signal detection in a fish with an epidermal lateral-line system. *Mar. Freshw. Res.* **57**, 611-617.
Bleckmann, H. and Münz, H. (1990). Physiology of lateral-line mechanoreceptors in a teleost with highly branched, multiple lateral lines. *Brain Behav. Evol.* **35**, 240-250.
Bleckmann, H., Waldner, I. and Schwartz, E. (1981). Frequency discrimination of the surface feeding fish *Aplocheilus lineatus* - a prerequisite for prey localization? *J. Comp. Physiol.* **143**, 485-490.

Bleckmann, H., Weiss, O. and Bullock, T. H. (1989). Physiology of the lateral line mechanoreceptive regions in the elasmobranch brain. *J. Comp. Physiol.* **164**, 459-474.

Budelmann, B. U. and Bleckmann, H. (1988). A lateral line analogue in cephalopods: water waves generate microphonic potentials in the epidermal head lines of *Sepia* and *Lolliguncula*. *J. Comp. Physiol. A* **164**, 1-5.

Clack, T. D. (1966). Effect of signal duration on the auditory sensitivity of humans and monkeys (*Macaca mulatta*). *J. Acoust. Soc. Am.* **40**, 1140-1146.

Coombs, S. and Janssen, J. (1990). Behavioral and neurophysiological assessment of lateral line sensitivity in the mottled sculpin, *Cottus bairdi*. *J. Comp. Physiol* **167**, 557-567.

Dehnhardt, G., Mauck, B. and Bleckmann, H. (1998). Seal whiskers detect water movements. *Nature* **394**, 235-236.

Dehnhardt, G., Mauck, B., Hanke, W. and Bleckmann, H. (2001). Hydrodynamic trail following in harbor seals (*Phoca vitulina*). *Science* **293**, 102-104.

Engelmann, J., Hanke, W. and Bleckmann, H. (2002). Lateral line reception in still- and running water. *J. Comp. Physiol.* **188**, 513-526.

Erbe, C., Reichmuth, C., Cunningham, K., Lucke, K. and Dooling, R. (2016). Communication masking in marine mammals: A review and research strategy. *Mar. Pollut. Bull.* **103**, 15-38.

Fletcher, H. (1940). Auditory patterns. *Rev. Mod. Phys.* **12**, 47-65.

Hanke, W., Witte, M., Miersch, L., Brede, M., Oeffner, J., Michael, M., Hanke, F., Leder, A. and Dehnhardt, G. (2010). Harbor seal vibrissa morphology suppresses vortex-induced vibrations. *J. Exp. Biol.* **213**, 2665-2672.

Hughes, G. M. (1966). The dimensions of fish gills in relation to their function. *J. Exp. Biol.* **45**, 177-195.

Kröther, S., Mogdans, J. and Bleckmann, H. (2002). Brainstem lateral line responses to sinusoidal wave stimuli in still and running water. *J. Exp. Biol.* **205**, 1471-1484.

Miersch, L., Hanke, W., Wieskotten, S., Hanke, F. D., Oeffner, J., Leder, A., Brede, M., Witte, M. and Dehnhardt, G. (2011). Flow sensing by pinniped whiskers. *Philos. Trans. R. Soc. B Biol. Sci.* **366**, 3077-3084.

Murphy, C. T., Eberhardt, W. C., Calhoun, B. H., Mann, K. A. and Mann, D. A. (2013). Effect of angle on flow-induced vibrations of pinniped vibrissae. *PLOS ONE* **8**, e69872.

Niesterok, B., Krüger, Y., Wieskotten, S., Dehnhardt, G. and Hanke, W. (2017). Hydrodynamic detection and localization of artificial flatfish breathing currents by harbour seals (*Phoca vitulina*). *J. Exp. Biol.* **220**, 174-185.

Popov, V. V. and Supin, A. Y. (1990). Auditory brain stem responses in characterization of dolphin hearing. *J. Comp. Physiol. A* **166**, 385-393.

Schulte-Pelkum, N., Wieskotten, S., Hanke, W., Dehnhardt, G. and Mauck, B. (2007). Tracking of biogenic hydrodynamic trails in a harbor seal (*Phoca vitulina*). *J. Exp. Biol.* **210**, 781-787.

Schwalbe, M. A. B., Sevey, B. J. and Webb, J. F. (2016). Detection of artificial water flows by the lateral line system of a benthic feeding cichlid fish. *J. Exp. Biol.* **219**, 1050-1059.

Tautz, J. and Sandemann, D. C. (1980). The detection of waterborne vibration by sensory hairs on the chelae of the crayfish. *J. Exp. Biol.* **88**, 351-356.

Westerweel, J. (1997). Fundamentals of digital particle image velocimetry. *Meas. Sci. Technol.* **8**, 1379-1392.

Wieskotten, S., Dehnhardt, G., Mauck, B., Miersch, L. and Hanke, W. (2010). The impact of glide phases on the trackability of hydrodynamic trails in harbour seals (*Phoca vitulina*). *J. Exp. Biol.* **213**, 3734-3740.